Journal of Catalysis

DISCOVERING THE ROLE OF SUBSTRATE IN ALDEHYDE HYDROGENATION

--Manuscript Draft--

Manuscript Number:	JCAT-20-2101R1
Article Type:	Research paper
Keywords:	Hydrogenation; hydrodeoxygenation; Pd; aromatic aldehyde; aliphatic aldehyde; adsorption; electron conjugation
Corresponding Author:	Laura Prati, PhD University of Milan Milano, ITALY
First Author:	Stefano Cattaneo
Order of Authors:	Stefano Cattaneo
	Sofia Capelli
	Marta Stucchi
	Filippo Bossola
	Vladimiro Dal Santo
	Eduard Araujo-Lopez
	Dmitry I. Sharapa
	Felix Studt
	Alberto Villa
	Alessandro Chieregato
	Bart D. Vandegehuchte
	Laura Prati, PhD
Abstract:	The hydrogenation and hydrodeoxygenation of aldehydes are important reactions in the field of catalysis for the synthesis of a wide range of chemicals. Pd-based catalysts are one of the most widely used class of catalysts for this purpose. Despite this, however, several aspects of their action mechanism still remain undisclosed, mainly due to the complexity of the surface chemistry involved, as well as the often ill-defined structure of the active sites. In this paper, we investigated in detail one of the critical parameters that governs the reactivity of the carbonylic group towards hydrogenation and hydrodeoxygenation: the effect of the side chain of aldehydes. Through the use of adsorption analyses and DFT study on two model molecules (benzaldehyde and octanal) we were able to exclude adsorption effects as a dominant factor ruling the reactivity of the carbonyl group. On the other hand, we found that a strong π-electron conjugation (such as a benzyl ring) is key in the conversion of aldehydes to alcohols and hydrocarbons, while molecules with no or weak π-electron conjugation (such as alkyl chains or single conjugated C=C double bond) remain inactive under the reaction conditions studied.

DISCOVERING THE ROLE OF SUBSTRATE IN ALDEHYDE HYDROGENATION

Stefano Cattaneo[a], Sofia Capelli[a], Marta Stucchi[a], Filippo Bossola[b], Vladimiro Dal Santo[b], Eduard Araujo-Lopez[c], Dmitry I. Sharapa[c], Felix Studt[c,d], Alberto Villa[a], Alessandro Chieregato[e], Bart D. Vandegehuchte[f] and Laura Prati[a,].*

[a] Dipartimento di Chimica, Università degli Studi di Milano, Via Golgi 19, 20133 Milano, Italy

[b] CNR – Istituto di Scienze e Tecnologie Chimiche "Giulio Natta", Via Golgi 19, 20133 Milano, Italy

[c] Institute of Catalysis Research and Technology, Karlsruhe Institute of Technology, Hermann-von-Helmholtz Platz 1, 76344 Eggenstein-Leopoldshafen, Germany

[d] Institute for Chemical Technology and Polymer Chemistry, Karlsruhe Institute of Technology, Engesserstrasse 18, 76131 Karlsruhe, Germany

[e] Total Research Center – Qatar (TRCQ), Qatar Science & Technology Park, Al Gharrafa, Doha P.O. Box 9803, Qatar

[f] Total Research & Technology Feluy, Zone Industrielle Feluy C, B-7181, Seneffe, Belgium

Abstract

The hydrogenation and hydrodeoxygenation of aldehydes are important reactions in the field of catalysis for the synthesis of a wide range of chemicals. Pd-based catalysts are one of the most widely used class of catalysts for this purpose. Despite this, however, several aspects of their action mechanism still remain undisclosed, mainly due to the complexity of the surface chemistry involved, as well as the often ill-defined structure of the active sites. In this paper, we investigated in detail one of the critical parameters that governs the reactivity of the carbonylic group towards hydrogenation and hydrodeoxygenation: the effect of the side chain of aldehydes. Through the use of adsorption analyses and DFT study on two model molecules (benzaldehyde and octanal) we were able to exclude adsorption effects as a dominant factor ruling the reactivity of the carbonyl group. On the other hand, we found that a strong π-electron conjugation (such as a benzyl ring) is key in the conversion of aldehydes to alcohols and hydrocarbons, while molecules with no or weak π-electron conjugation (such as alkyl chains or single conjugated C=C double bond) remain inactive under the reaction conditions studied.

Introduction

The field of catalysis has revolutionised the chemical industry over the past 150 years such that nowadays over 70 % of all chemical industrial processes rely on heterogeneous catalysis.[1,2] Although heterogeneous catalysis can be considered an old discipline, the research is not stagnating; new catalysts and processes are constantly being developed.[3] However, the complexity of the surface chemistry involved, as well as the often ill-defined structure of the active sites, render the study of fundamental aspects within heterogeneous catalysis challenging.[4,5] For example, in the Haber-Bosch process for the synthesis of ammonia (the most important chemical manufacturing process in the world), there is still a gap between theoretical calculations and lab-scale tests and the actual industrial process.[6] This prevents straightforward extrapolation of results based on theoretical calculations to the industrial process.[7]

Supported metal nanoparticles have attracted growing attention in the last few decades as active and selective catalysts for several reactions of industrial interest.[8,9] The hydrogenation and hydrodeoxygenation of aldehydes, in particular, are important industrial processes for the production of a wide range of chemicals that find use as solvents, fuels, plasticisers, detergents, pharmaceutical precursors and fine chemicals.[10–12] Aldehydes, in fact, can be found in several biomass-derived feedstock; 5-hydroxymethylfurfural and furfural, for example, are the products of dehydration of fructose and xylose respectively, while vanillin can be found in the complex lignin structure.[13–15] For this reason, the conversion of aldehydes is nowadays playing a crucial role, as the valorisation of biomass-derived compounds is a critical step towards the replacement of fossil fuel as source of chemicals.[16]

A vast body of work is reported in the literature regarding the hydrogenation and hydrodeoxygenation of aldehydes using Pd-based heterogeneous catalysts. Pd, in fact, is considered a suitable catalyst for these types of reactions due to its capacity to dissociate and easily activate molecular hydrogen.[17] However, several aspects of the reaction mechanism of Pd-based catalysts still remain unclear. For example, the scientific literature is still vague on the effect of the side chain of aldehydes in the hydrogenation and hydrodeoxygenation of the carbonyl group. The physico-chemical properties of the substituent group on aldehydes, in fact, can strongly affect its reactivity in several ways, such as by increasing/decreasing the substrate adsorption (or modifying its geometry) through steric effects or by increasing/decreasing the electronic density on the carbonyl bond.

A steric effect was first addressed by Kobayashi et al. using cyclohexanone and one of its methyl-substituted derivatives (2-, 3-, or 4-methylcyclohexanone) as model substrates.[18] The results clearly showed that the methyl-substituted ketones were less reactive than cyclohexanone over different metal catalysts (including Pd), and the decreased reactivity was ascribed to a steric hindrance of the methyl group towards the adsorption of the substrate on the catalyst surface. Moreover, Santori and colleagues observed a higher hydrogenation rate of benzaldehyde with respect to butyraldehyde over Pt-based catalysts, attributing the phenomenon to the lower strength of the C=O bond in aromatic aldehydes with respect to aliphatic ones.[19] Kieboom also reported that hydrodeoxygenation is accelerated by electron-donating groups on the aromatic ring of benzyl alcohol derivatives over Pd-based catalysts.[20] Different results were, however, reported by Keane et al., who noticed a decreased rate for the hydrogenation of 2-methylbenzaldehyde compared to benzaldehyde over a Ni-based catalyst and ascribed this effect to the electron-donating property of the methyl group in *ortho* position[21]

One of the fundamental steps in heterogeneous catalysis is the adsorption of the substrate on the active site. In the case of molecules containing a carbonylic group such as aldehydes, the adsorption can happen in two modes: η_1–(O) mode and η_2-(C, O) mode.[22] The former implies the interaction between the lone pair of oxygen with the catalyst surface, while the latter involves the interaction with the double bond of the carbonyl group. These adsorption modes are affected not only by steric hindrance but also by electronic effects. In the case of furfural and 5-hydroxymethylfurfural, for example, a strong interaction between the catalyst and the π-bonds of the aromatic furan ring directs the adsorption of the substrate to a flat η_2-(C, O) position.[23] This, in turn, can strongly affect the selectivity of the reaction, increasing the rate of side reactions such as decarbonylation and furan ring hydrogenation, as demonstrated by Duarte et al.[24]

It is therefore clear that despite the paramount importance of hydrogenation and hydrodeoxygenation reactions, fundamental studies on parameters that rule the reactivity of the carbonyl group are limited and they often lack in considering the catalytic system as a single ensemble constituted by catalyst (metal and support) and substrate.

This work presents a systematic analysis of the main roles played by the nature of carbonyl-bearing substrates in hydrogenation and hydrodeoxygenation reactions on Pd-based catalysts, with the aim to shed light on their entangled mechanisms. By selecting aromatic and aliphatic aldehydes differing not only in

structure but also in electron density of the carbonyl group, we could study: (i) the substrate adsorption, which in turn is an indication of the proximity of the substrate to the active site and its retention by the catalyst; (ii) the electronic structure of the reducible group (C=O), which interacts with the electronic properties of the catalytic site. These two effects were studied using a combination of analytical tools (such as N_2 and substrate adsorption and temperature programmed desorption analysis) and theoretical models (density functional theory studies) and catalytic tests. We believe that this study can unravel the main factors governing the reaction mechanism, providing a guideline for the future synthesis of materials with high activity and selectivity in the framework of hydrogenation/hydrodeoxygenation of aldehydes.

Experimental

Materials

K_2PdCl_4 (99.99 %, Merck) was used as metal precursor, and commercial activated carbon (Norit Carbon GSX, hereafter referred as "AC") was used as support. $NaBH_4$ (99.99 %, Merck) and poly(vinyl alcohol) (PVA, M_w = 9000 – 10000, 80 % hydrolysed, Merck) were used for the catalyst preparation. Benzaldehyde (99 %, Merck), n-octanal (99 %, Merck), trans-2-octenal (95 %, Merck), cyclohexanecarboxaldehyde (97 %, Merck), cinnamaldehyde (99 % Merck), cinnamyl alcohol (98 %, Merck), hydrocinnamaldehyde (98 %, Merck) and phenylacetaldehyde (95 %, Merck) were used as substrates. p-xylene (99 %, Merck) was used as solvent.

Catalyst preparation

The Pd/AC catalyst was synthesised following a sol-immobilisation procedure. To an aqueous solution of K_2PdCl_4 of the desired concentration (total metal concentrations of 1 mmol L^{-1}), a PVA solution (1 wt%) was added (PVA/Pd) (w/w) = 0.5) under constant stirring. A freshly prepared aqueous solution of $NaBH_4$ (0.1 M, $NaBH_4$/Pd (mol/mol) = 8) was then added to form a dark-brown sol. After 30 minutes of sol generation, the colloid was immobilised by adding the support and acidified to pH 2 with sulfuric acid under continuous vigorous stirring. The amount of support material required was calculated to have a total final metal loading of 1 wt%. After 1 h of stirring, the slurry was filtered and the catalyst was washed thoroughly with 1 L of distilled water and dried at 80 °C for 4 h.

Catalyst characterisation

Transmission electron microscopy (TEM) analysis of the supported Pd nanoparticles was carried out with a ZEISS LIBRA 200FE microscope equipped with a 200 kV FEG source. The specimens were finely smashed in an agate mortar, suspended in isopropanol (99.8 %, Merck) and sonicated, then each suspension was dropped onto a lacey carbon-coated copper grid (300 mesh) and the solvent was evaporated. Histograms of the particle size distribution were obtained by counting at least 500 particles. The mean particle diameter (d_m) was calculated using the formula $d_m = \sum d_i n_i / n_i$, where n_i is the number of particles with diameter d_i.

X-ray photoelectron spectra (XPS) were acquired in an M-probe apparatus (Surface Science Instruments) equipped with an atmospheric reaction chamber. The XPS line of Pd 3d was recorded by applying an Al Kα characteristic X-ray line and (hv = 1486.6 eV) pass energy. All data were analysed using CasaXPS (Microsoft Corporation, v2.3.17 PR1.1).

All isotherms were collected with an ASAP2020 instrument (Micromeritics). Prior to each analysis, the samples were degassed under high vacuum for 5 h at 110 °C. The nitrogen adsorption isotherms were

collected at -196 °C, while those with benzaldehyde and octanal at 50 °C up to about 2 mmHg of absolute pressure. The micropores distribution is reported as pore width vs $dA/d\log(W)$ and was calculated considering slit-like pores by using the NLDFT(SD3), N2-77-Carbon Slit Pores DFT method provided by Micromeritics.

Temperature Programmed Desorption (TDP) analyses of benzaldehyde and octanal were performed with a home-made gas feeding apparatus described elsewhere[25] and connected downstream to a mass spectrometer (Hiden, HPR). The catalysts (50 mg) were loaded in a U-shaped quartz reactor and before each analysis, they were treated for 1 h at 110 °C under He flow (40 mL min^{-1}). After cooling the reactor to 75 °C, the adsorption of the substrates was carried out by flowing the He carrier gas (40 mL min^{-1}) through a saturator at 40 °C. After adsorption, the reactor was purged until no mass signal of the substrates was detected. The TPD analysis was performed by heating up the reactor to 350 °C with at 5 °C/min rate.

Computational Details

Density functional theory (DFT) calculations were carried out using the Vienna Ab Initio Simulation Package (VASP)[26,27] and the Atomic Simulation Environment (ASE)[28] employing the generalised gradient approximation (GGA) with Bayesian error estimation functional with van der Waals corrections (BEEF-vdW)[29,30] and the projector-augmented wave (PAW) potentials.[31,32] The computational setup is similar as in previous work.[33] Briefly, a four-layer slab of palladium with varying supercell sizes and *k*-point meshes were used (see Table S1). During the relaxations, the two bottom layers of the slabs were kept fixed at the bulk positions. A kinetic energy cutoff of 450 eV was used for all calculations. In order to avoid interaction between periodic images, the Pd slabs are separated by approximately 20 Å of vacuum along the *z*-direction.

We performed additional, single-point energy calculations using the PBE functional, including Grimme's dispersion corrections (PBE-D3, zero damping).[34,35]

The adsorption energy is defined as follows:

$$E_{ads} = E_{X+surf} - E_X + E_{surf} \quad (1)$$

In Equation (1), all energies refer to systems with optimised structures; E_{X+surf} stands for the total energy of the molecule/species adsorbed, E_X is the energy of the adsorbate calculated in the gas phase, and E_{surf} is the energy of the slab. By this definition, a negative value implies an exothermic process and indicates and stable adsorption. The isolated molecules were structurally relaxed inside a large simulation box of 20×20×20 $Å^3$.

Catalytic tests

Catalytic reactions were carried out in a 100 mL stainless steel autoclave equipped with a glass inlet. In a typical experiment, 10 mL of a 0.3 mol L^{-1} solution of substrate in *p*-xylene and an appropriate amount of catalyst (substrate : Pd molar ratio of 1000 : 1) were placed into the glass inlet along with a magnetic stirrer. The autoclave was sealed and flushed several times with N_2 first in order to remove any residual oxygen in the atmosphere and then pressurised at the desired H_2 pressure (typically 2 bar). The autoclave was then heated up to the desired temperature (typically 50 °C) and the reaction mixture stirred at a constant stirring rate of 1000 rpm. Samplings were carried out by stopping the stirring and quenching the reaction under cold water. 200 µL of the reaction mixture was withdrawn under stirring for not altering the catalyst/reagent ratio and then centrifuged in order to separate the catalyst. 100 µL of the supernatant solution was then diluted with a solution of 1-dodecanol in *p*-xylene (external standard) for GC measurement. Product analysis and quantification were carried out with a GC-FID equipped with a non-polar column (Thermo Scientific, TRACE 1300 equipped with an Agilent HP-5 column).

Results and discussion

Catalyst synthesis and characterisation

The reactivity of the carbonyl group (C=O) towards hydrogenation and hydrodeoxygenation can be affected by the carbon structure bearing the functional group. In order to study the impact that different side chain have on carbonyl reactivity, we employed a single benchmark catalyst throughout this study, namely 1 wt% Pd on activated carbon (Pd/AC). This way, any possible uncontrolled variable caused by the nature of the catalyst (such as particle size, morphology, support, etc.) is avoided. The catalyst was synthesised by a traditional sol-immobilisation technique following a protocol developed by Prati and co-workers (see Experimental section).[36,37] This method allows great control over average particle size and particle size distribution.

The Pd nanoparticles in the sol were quantitatively deposited onto the support as confirmed by ICP analysis of the filtrate solution (no Pd was detected, therefore we assumed that the actual Pd loading corresponded to the nominal loading). TEM analysis was performed on the final catalyst, showing Pd particles homogeneously dispersed which exhibited a mean particle size of 4.1 ± 1.3 nm (Figure 1 - left). XPS analysis was performed in order to evaluate the oxidation state of the deposited Pd nanoparticles. From peak deconvolution of the Pd 3d orbital (Figure 1 - right), 80 % of the Pd at the surface resulted in the zero-valent oxidation state, while the remaining 20 % was in the form of Pd^{2+}.

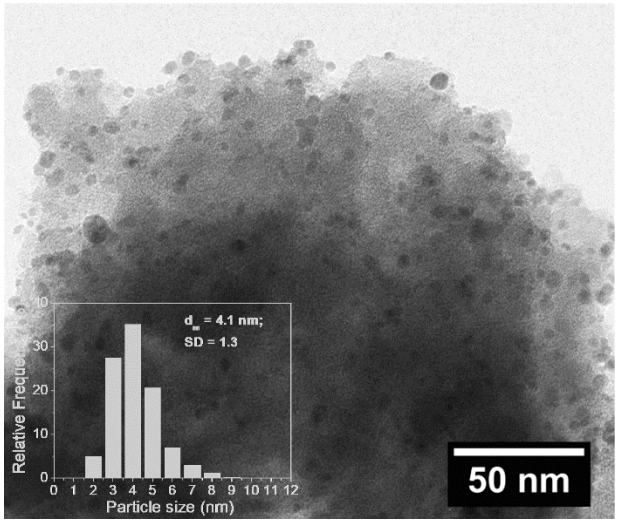

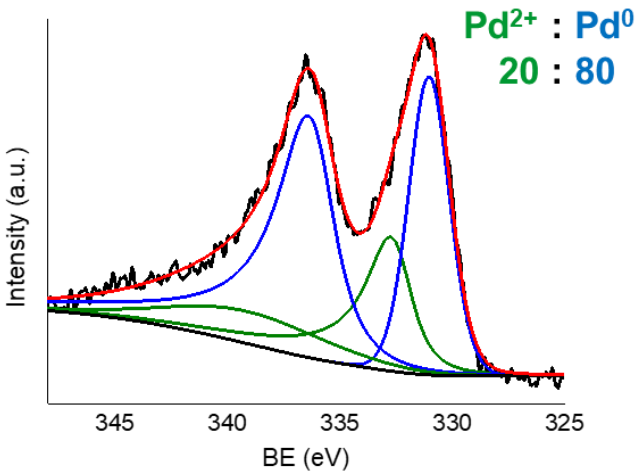

Figure 1: *Characterisation of the 1 wt% Pd/AC catalyst: (left) TEM analysis with relative particle size distribution and (right) XPS analysis of the Pd 3d orbital with Pd(II) and Pd(0) relative abundance.*

Nitrogen adsorption isotherms were recorded for the bare carbon support and for the Pd/AC catalyst (Figure 2) in order to evaluate possible surface changes induced by the immobilisation of Pd nanoparticles. As shown by the results in Figure 2 - left, the two nitrogen physisorption isotherms are quite similar in shape and, specifically, are of Type IV with a hysteresis tentatively of Type H4 according to the IUPAC classification. This means that both the materials are of microporous nature and do not present mesopores, with the hysteresis loop that is reminiscent to narrow slit-like pores.[38]

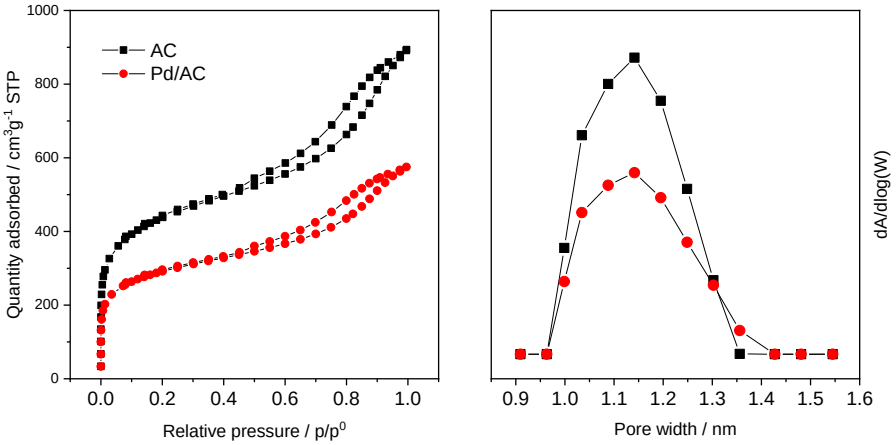

Figure 2: *Nitrogen adsorption isotherms (left) and micropore distribution as pore width vs dA/dlog(W) of AC and Pd/AC.*

The total specific surface area of the AC sample (1441 $m^2\ g^{-1}$) is common for activated carbons, with about 500 $m^2\ g^{-1}$ due to microporosity. The total pore volume is 1.19 $cm^3\ g^{-1}$ of which 0.26 $cm^3\ g^{-1}$ are due to the micropores. These values respectively decrease about 30 % upon Pd nanoparticle immobilisation, with the Pd/AC sample showing 950 $m^2\ g^{-1}$ of specific surface area and 366 $m^2\ g^{-1}$ of micropore area. We note that the decrease in micropore volume and area is similar to the decrease in external surface area (about 30 %). Nonetheless, the relative distribution of micropores is unaltered between the two samples (Figure 2 - right) and only their absolute concentration is affected (Table 1). This indicates the preferential deposition of Pd on the external surface of the carbon support, rather than within the micropores. It is therefore reasonable to assume that differences in the adsorption capacity between the two samples are due to factors other than microporosity.

Table 1: *Specific surface areas and pore volumes of AC and Pd/AC.*

Sample	Specific Area ($m^2\ g^{-1}$)			Volume ($cm^3\ g^{-1}$)	
	Total	Micropores	External	Total	Micropores
AC	1441	499	942	1.19	0.26
Pd/AC	950	366	584	0.74	0.20

Hydrogenation/hydrodeoxygenation of aldehydes

In order to establish the influence of the aldehyde structure on the catalyst behaviour, benzaldehyde and n-octanal were first chosen as representative of an aromatic and of an aliphatic aldehyde. Figure 3 shows the products expected from hydrogenation/hydrodeoxygenation of the two substrates. The reactions were firstly performed under mild conditions (50 °C, 2 bar of H_2 and a substrate-to-metal ratio of 1000 : 1), using a non-polar solvent (p-xylene).

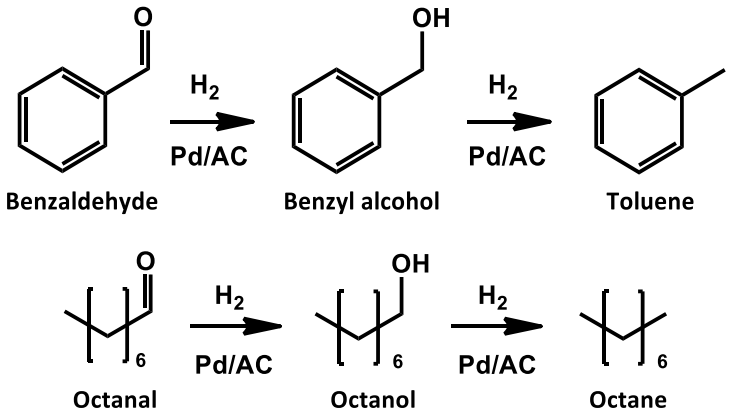

Figure 3: *Possible reaction pathway for the hydrogenation/hydrodeoxygenation of (top) benzaldehyde and (bottom) n-octanal.*

When benzaldehyde was used as the substrate, almost full conversion was obtained in only 1 hour (95 % conversion, with an initial activity calculated at 15 minutes of 0.21 mol L^{-1} h^{-1}), with most of the reaction product being benzyl alcohol (Figure 4, 86 % selectivity). The produced alcohol was then further fully converted into toluene after 2 additional hours (Figure S1). The reaction profile clearly highlights the consecutive behaviour of the two reactions (hydrogenation and hydrodeoxygenation).

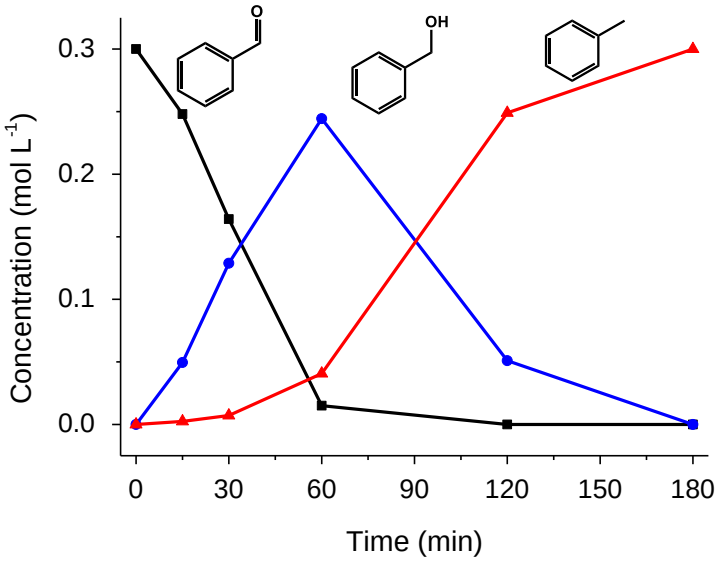

Figure 4: *Benzaldehyde hydrogenation/hydrodeoxygenation reaction. Reaction conditions: 50 °C, 2 bar of H_2, substrate-to-metal ratio 1000 : 1, benzaldehyde 0.3 mol L^{-1} in p-xylene.*

Using n-octanal under the same reaction conditions, however, no activity of the catalytic system was observed, even after extended reaction time (5 h). The reaction temperature and hydrogen pressure were then increased up to 150 °C and 20 bar, respectively, but again no products of hydrogenation or hydrodeoxygenation (when octanol was used as substrate) were observed. We finally used cyclohexane and ethanol as a solvent, but also in this case no significant change in activity was noticed, allowing us to exclude a possible solvent effect (i.e. competitive adsorption between solvent and substrate).

It is therefore clear that the nature of the carbon backbone plays a crucial role in the substrate reactivity. This behaviour might be due to lack of interaction between octanal and the catalyst surface, to an intrinsically

different electron density of the carbonyl group, or to both. In order to elucidate the main factor influencing this type of reaction, we continued the study via a combination of density functional theory calculations (adsorption energies) and catalytic tests (adsorption and electronic effects).

Adsorption effect

One of the reasons why octanal does not show conversion might be that it does not interact with the catalyst surface. With this in mind, we performed adsorption isotherms using benzaldehyde and n-octanal as probe substrates. Interestingly, increasing the substrate partial pressure both benzaldehyde and octanal interact with the catalyst surface (Figure 5). A higher amount of benzaldehyde was adsorbed at any time compared to octanal, with a maximum quantity adsorbed of 66 $cm^3\ g^{-1}$ (compared to 62 $cm^3\ g^{-1}$ with octanal) before condensation phenomena occur at ca. 2.0 mmHg. In addition, the adsorption isotherms of the two substrates follow a different trend in the whole pressure range studied, which suggests a different adsorption mechanism for the two molecules. In particular, the isotherm of octanal changes slope more than once in the range of pressures studied. This means that the mechanism of adsorption of octanal is more complex than benzaldehyde and/or might involve different adsorption sites as highlighted in the DFT study (see below).

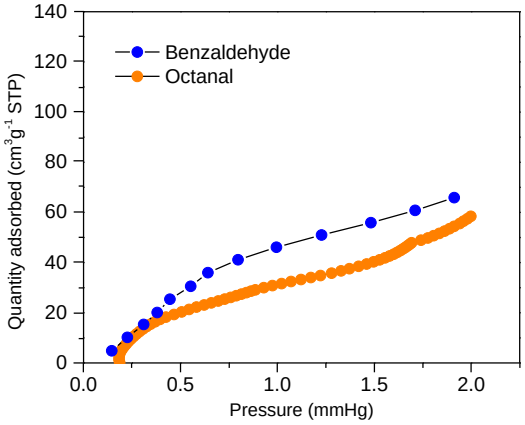

Figure 5: *Benzaldehyde and octanal adsorption isotherms of Pd/AC.*

Adsorption isotherms showed that octanal (as well as benzaldehyde) adsorbs on the catalyst surface. In particular, the reactants are likely to adsorb mainly within the carbon micropores; micropores, in fact, have a strong interaction with the substrates due to weak Van der Waal interactions. This technique, however, does not provide information regarding the strength of interaction between the different substrates and the catalyst surface. For this reason, we carried out temperature programmed desorption (TPD) measurements using both benzaldehyde and octanal as probe molecules for the Pd/AC catalyst (Figure 6). Although the peak areas cannot be directly compared, as it was impossible to calibrate the mass spectrometer due to the very low vapour pressure of both molecules, the chemisorption of octanal was proven by the presence of substrate desorbing at a temperature of 140 °C (orange line). Benzaldehyde desorbed at a similar temperature (133 °C), showing in this case a much stronger signal (blue line). These low desorption temperatures obtained point in the direction of substrate physisorption onto the catalyst surface.

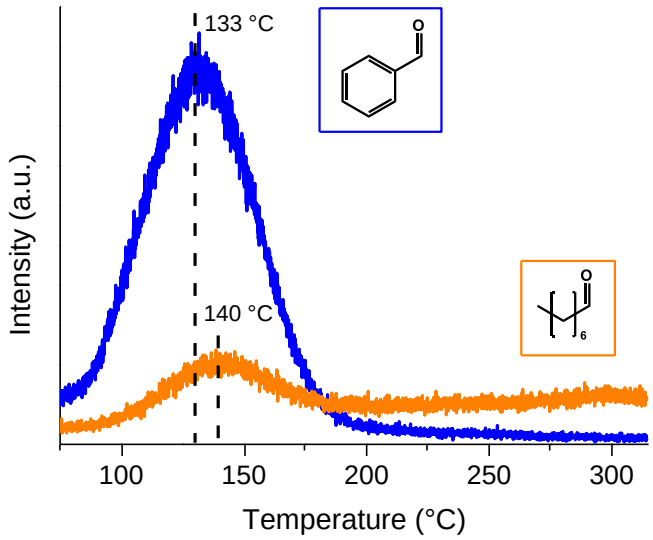

Figure 6: *TPD analysis of benzaldehyde and octanal on the Pd/AC catalyst.*

In order to understand and quantify the differences in adsorption strengths between the two substrates, density functional theory (DFT) calculations were carried out. A benchmarking of common density functionals for the calculations of benzaldehyde and octanal was initially performed due to the difficult description of the interaction of benzaldehyde and octanal with transition metal surfaces (see SI). Briefly, we quantified our DFT calculations using experimental data for (1) the adsorption of linear alkanes on Pd(111) surfaces[39] and (2) the adsorption of benzene on Pd(111).[40] As shown in Figure S2, while PBE-D3 performs well for the adsorptions of alkanes on Pd(111), BEEF-vdW severely underestimates their adsorption energies. Contrary, BEEF-vdW is performing rather well for benzene adsorption on Pd(111), while PBE-D3 is not. We therefore employ the PBE-D3 and BEEF-vdW functionals for our investigations of the adsorption of octanal and benzaldehyde, respectively.

The adsorption energies of octanal (calculated with PBE-D3) and benzaldehyde (calculated with BEEF-vdW) as a function of surface coverage are shown in Figure 7a. In both cases, the adsorption energy depends on the coverage. At low coverage (one molecule in a 3x7 unit cell of Pd(111) corresponding to a coverage of θ = 0.007 molecules per Å^2), octanal is chemisorbed on the palladium surface through a η_1–(O) mode, and the aliphatic chain lays down on the surface with an adsorption energy of -138 kJ/mol (see Figure 7b, structure A). As the coverage increases (one molecule per 3x2 and 2x2 unit cells), the octanal molecules start to tilt over, reducing the adsorption energy to -97 kJ/mol (see Figure 7b, structure C).

Benzaldehyde adsorbs with the aromatic ring parallel to the Pd(111) surface in an almost flat geometry with an adsorption energy of about -120 kJ/mol at low coverages, θ = 0.007 and 0.009 molecules/Å^2 (which correspond to 4x5 and 4x4 unit cells, see Figure 7b, structure D). Higher coverages were evaluated with a single molecule in 3x2 and 2x2 unit cells of Pd(111) surface, θ = 0.024 and 0.036 molecules/Å^2 respectively. At θ = 0.024, the benzaldehyde molecules adsorb through a η_2–(O) mode (see Figure 7b, structure E) with an energy of -66 kJ/mol. A decrease of more than half of the adsorption energy is found at high coverage of benzaldehyde (*ca.* -54 kJ/mol) (see Figure 7b, structure F). The adsorption energies of octanal are always higher than those for benzaldehyde at any coverage investigated herein, confirming the results obtained by TPD.

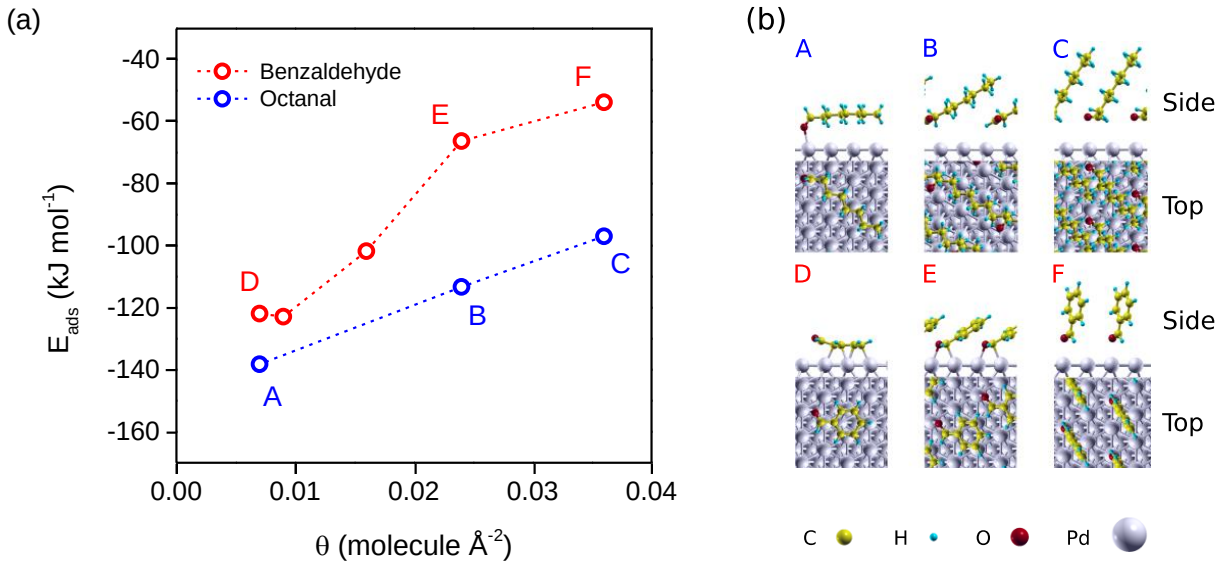

Figure 7: *(a) Octanal and benzaldehyde adsorption energies as a function of the surface coverage. (b) Configurations of the octanal (A, B, and C) and benzaldehyde (D, E, and F) adsorptions. Coverages are given as molecules per Å² of the Pd surface.*

From the theoretical and experimental results, we therefore conclude that both substrates change adsorption mechanisms depending on the surface coverage. When normalising the adsorption energies to the number of molecules per surface area of Pd (molecules/Å^2), we find that octanal binds more strongly to the Pd surface compared to benzaldehyde over the range of coverages investigated herein.

The results of DFT calculations fit perfectly with TPD and adsorption isotherm results, but the differences revealed in adsorption energy between the two substrates are not enough to justify the complete inactivity of octanal hydrogenation on the Pd/AC catalyst. Octanal, in fact, is completely inactive at any range of concentration, while benzaldehyde can be easily converted. Despite the adsorption of the substrate on the catalyst surface is one of the catalytic step of the reaction, it is clear that in this specific instance it is not the ruling factor determining the final catalytic activity. To fully investigate the systems and highlight the possible role of carbonyl electron density we carried out a set of experiments using slightly different substrates which differ from each other in electron density of the carbonyl group.

Electronic effect

Different substrates were tested under the same reaction conditions (50 °C, 2 bar of H_2 and a substrate-to-metal ratio of 1000 : 1). Firstly, we employed cyclohexanecarboxaldehyde and 2-octenal (Figure S3). The former is similar in structure to benzaldehyde but has the aromatic ring fully hydrogenated, eliminating the conjugation between the aromatic ring and the carbonyl group. The latter molecule is structurally similar to *n*-octanal but contains an additional double bond conjugated to the carbonyl bond (α,β-unsaturated aldehyde, enal).

The catalytic results show no conversion at all when using cyclohexanecarboxaldehyde, while 100 % of conversion was obtained with 2-octenal after 2 h (initial activity of 0.31 mol L^{-1} h^{-1}), yielding n-octanal as the only product (therefore only the C=C bond was hydrogenated) (Figure 8). The C=C bond hydrogenation is thermodynamically favoured over the C=O bond hydrogenation. In both cases, however, the carbonyl group was not affected. Excluding significant differences in adsorption energy between octanal and octenal, the hydrogenation of the double bond rapidly transforms octenal in octanal, which was earlier found inactive

under these conditions. The inactivity of cyclohexanecarboxaldehyde further suggests that the presence of a stable π-electron conjugation is a prerequisite for the reduction of the carbonyl group.

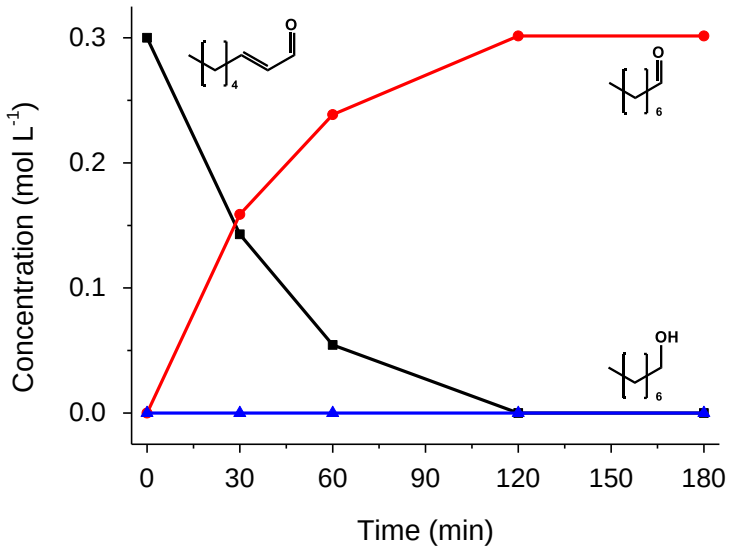

Figure 8: *2-octenal reaction profile. Reaction conditions: 50 °C, 2 bar of H_2, substrate-to-metal ratio 1000 : 1, 2-octenal 0.3 mol L^{-1} in p-xylene.*

To confirm this latter statement, cinnamaldehyde was employed representing a substrate containing a conjugated system with both an aromatic ring and a simple C=C bond. The catalytic results (Figure 9) show the formation of hydrocinnamaldehyde (C=C hydrogenation) as the major product (ca. 80 % of selectivity) and hydrocinnamyl alcohol (both C=C and C=O hydrogenation) as the side-product (ca. 20 % of selectivity; combined initial activity of 0.07 mol L^{-1} h^{-1}); no hydrodeoxygenation products were detected. It is clear that the hydrogenation of the double bond is favoured compared to the hydrogenation of the carbonyl group, but the presence of hydrocinnamyl alcohol in the reaction mixture demonstrates that also the carbonyl group can be reduced. Hydrocinnamyl alcohol can be formed following two different pathways which greatly differ from a mechanistic point of view, as presented in Figure 10: the first one consists of a C=O hydrogenation step followed by C=C reduction, while the second pathway consists of a first hydrogenation of the C=C bond followed by reduction of the carbonyl. In the first pathway, C=O hydrogenation takes place in the presence of a conjugated system, while in the other the carbonyl group is isolated but still in the presence of an aromatic ring which can contribute to have a similar adsorption energy as benzaldehyde. Since no cinnamyl alcohol production was observed at any point, the small amount of hydrocinnamyl alcohol formed and the fast double bond hydrogenation suggest that hydrocinnamyl alcohol is formed through the first pathway (1. carbonyl hydrogenation, 2. double bond reduction). This hypothesis was confirmed experimentally by using hydrocinnamaldehyde as substrate: in this case, no conversion was observed (Table 2). On the other hand, using cinnamyl alcohol as the substrate full conversion to hydrocinnamyl alcohol was obtained after less than 2 h of reaction, thus confirming that C=C bond hydrogenation is very fast. A similar behaviour was observed in the case of the hydrodeoxygenation reaction. As expected, in fact, using hydrocinnamyl alcohol as the substrate led to no conversion into phenylpropare, since once again the substrate does not have a stable π-electron system conjugated to the OH group.

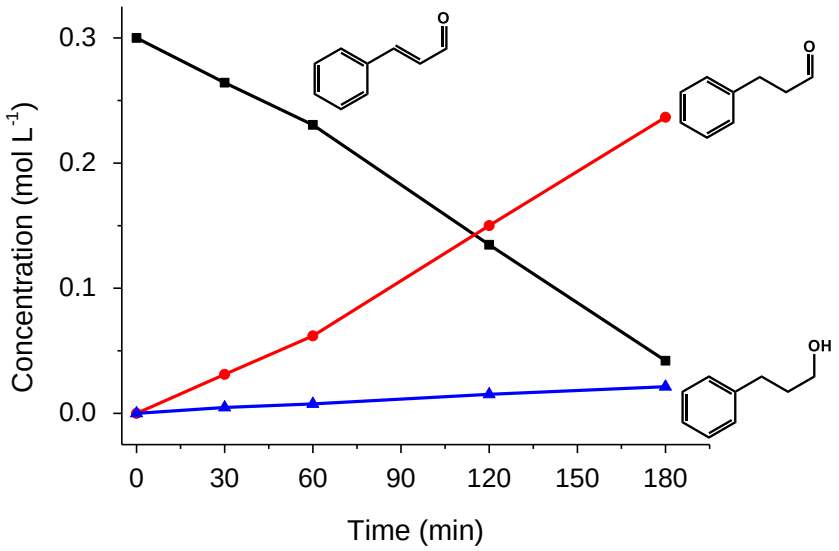

Figure 9: *Cinnamaldehyde reaction profile. Reaction conditions: 50 °C, 2 bar of H_2, substrate-to-metal ratio 1000 : 1, cinnamaldehyde 0.3 mol L^{-1} in p-xylene.*

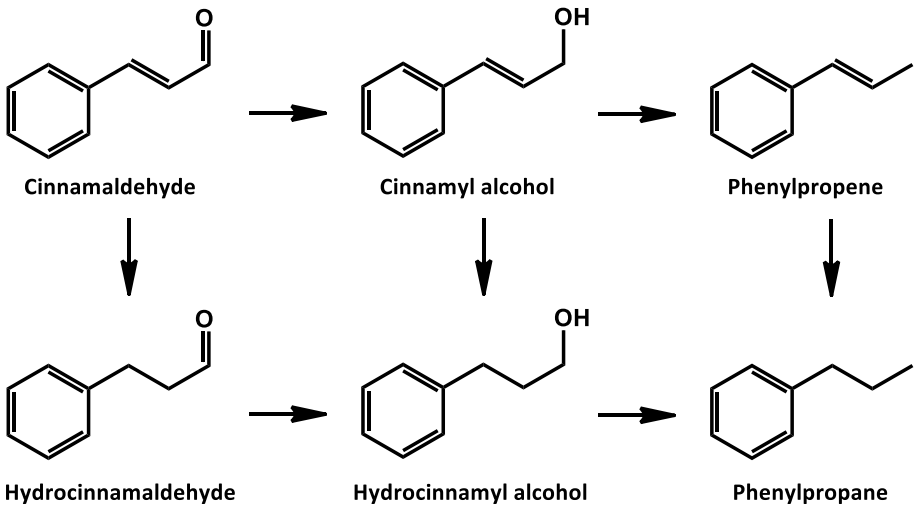

Figure 10: *Possible reaction pathways for the hydrogenation/hydrodeoxygenation of cinnamaldehyde.*

Table 2: *Catalytic tests performed using hydrocinnamaldehyde, cinnamyl alcohol and hydrocinnamyl alcohol as starting material. Reaction conditions: 50 °C, 2 bar of H_2, substrate-to-metal ratio 1000 : 1, substrate 0.3 mol L^{-1} in p-xylene, reaction time 2 h.*

Substrate	Conversion (%)	Selectivity hydrocinnamyl alcohol (%)	Selectivity phenylpropane (%)
Hydrocinnamaldehyde	0	-	-
Cinnamyl alcohol	100	> 99	< 1
Hydrocinnamyl alcohol	0	-	-

Based on these results, we demonstrated the role of the aromatic ring in activating the carbonyl group of aldehydes. The addition of a C=C conjugation between the aromatic ring and the carbonyl group maintains

the ability to activate the aldehyde towards hydrogenation, as confirmed by the small amount of hydrocinnamyl alcohol detected. The rate of C=C hydrogenation, however, is much faster than the carbonyl reduction on Pd surface due to thermodynamic reasons.

A conclusive experiment was carried out using phenylacetaldehyde where only one carbon atom separates the aromatic ring from the carbonyl bond (Figure S4). In this case no conversion was obtained, confirming that the absence of CHO conjugation inhibits C=O reduction even in the presence of the aromatic ring.

Conclusions

In this work we elucidated the factors affecting the hydrogenation and hydrodeoxygenation of various aldehydes on a Pd-based catalyst. By using benzaldehyde and *n*-octanal, we demonstrated the importance of the side chain in determining the reactivity of carbonyl group. Although the adsorption mode and strength are affected by the structure of the substrate, these aspects have proven not to be the decisive factors in the conversion of the carbonyl group. This was demonstrated by a combination of adsorption studies (N_2 and substrates adsorption, as well as temperature programmed desorption), theoretical models (density functional theory studies), and dedicated experiments. Electronic activation of the carbonyl group via strong π-electron conjugation, as found in a benzyl ring, was found key in the conversion of aldehydes to alcohols and hydrocarbons, while molecules with no or weak π-electron conjugation (such as alkyl chains or single conjugated C=C double bond) remain inactive under the reaction conditions studied.

In addition, we believe that this study can provide useful guidelines for the future synthesis of materials with high activity and selectivity in the framework of hydrogenation/hydrodeoxygenation of aldehydes. Moreover, a similar approach of study could be extended to other substrates and reactions, further increasing our knowledge on the mechanisms that govern heterogeneous catalysis.

Declaration of competing interest

The authors declare that they have no known competing financial interests or personal relationship that could have appeared to influence the work reported in this paper.

Acknowledgments

The authors acknowledge the Total “Consortium on Metal Nanocatalysis” project for the funding. Total Research Center Qatar is gratefully acknowledged for the coordination of the collaboration.

References

1 J. Sá and J. Szlachetko, *Catal. Letters*, 2014, **144**, 197–203.

2 J. Hagen, *Industrial Catalysis: A Practical Approach*, Wiley, Third Edit., 2015.

3 P. Lanzafame, S. Perathoner, G. Centi, S. Gross and E. J. M. Hensen, *Catal. Sci. Technol.*, 2017, **7**, 5182–5194.

4 K. I. Tanaka, *Catal. Today*, 2010, **154**, 105–112.

5 J. A. Hedvall, *Adv. Catal.*, 1956, **8**, 1–15.

6 T. Kandemir, M. E. Schuster, A. Senyshyn, M. Behrens and R. Schlögl, *Angew. Chemie - Int. Ed.*, 2013,

52, 12723–12726.

7 A. Corma, *Angew. Chemie - Int. Ed.*, 2016, **55**, 6112–6113.

8 S. Cattaneo, M. Stucchi, A. Villa and L. Prati, *ChemCatChem*, 2019, **11**, 309–318.

9 M. J. Ndolomingo, N. Bingwa and R. Meijboom, *J. Mater. Sci.*, 2020, **55**, 6195–6241.

10 P. Gallezot and D. Richard, *Selective Hydrogenation of α,β-Unsaturated Aldehydes*, 1998, vol. 40.

11 J. wei Zhang, K. kang Sun, D. dan Li, T. Deng, G. ping Lu and C. Cai, *Appl. Catal. A Gen.*, 2019, **569**, 190–195.

12 D. Procházková, P. Zámostný, M. Bejblová, L. Červený and J. Čejka, *Appl. Catal. A Gen.*, 2007, **332**, 56–64.

13 S. Cattaneo, D. Bonincontro, T. Bere, C. J. Kiely, G. J. Hutchings, N. Dimitratos and S. Albonetti, *ChemNanoMat*, 2020, **6**, 1–8.

14 S. Alijani, S. Capelli, S. Cattaneo, M. Schiavoni, C. Evangelisti, K. M. H. Mohammed, P. P. Wells, F. Tessore and A. Villa, *Catalysts*, 2020, **10**, 1–16.

15 S. Alijani, S. Capelli, C. Evangelisti, L. Prati, A. Villa and S. Cattaneo, *Catal. Today*, , DOI:10.1016/j.cattod.2020.04.026.

16 H. Zang, K. Wang, M. Zhang, R. Xie, L. Wang and E. Y.-X. Chen, *Catal. Sci. Technol.*, 2018, **8**, 1777–1798.

17 S. Nishimura, *Handbook of heterogeneous catalytic hydrogenation for organic synthesis*, 2001.

18 K. Tanaka, Y. Takagi, O. Nomura and I. Kobayashi, *J. Catal.*, 1974, **35**, 24–33.

19 G. F. Santori, M. L. Casella and O. A. Ferretti, *J. Mol. Catal. A Chem.*, 2002, **186**, 223–239.

20 A. P. G. Kieboom, J. F. De Kreuk and H. Van Bekkum, *J. Catal.*, 1971, **20**, 58–66.

21 M. A. Keane, *J. Mol. Catal. A Chem.*, 1997, **118**, 261–269.

22 R. Shekhar, M. A. Barteau, R. V. Plank and J. M. Vohs, *J. Phys. Chem. B*, 1997, **101**, 7939–7951.

23 S. Chen, R. Wojcieszak, F. Dumeignil, E. Marceau and S. Royer, *Chem. Rev.*, 2018, **118**, 11023–11117.

24 D. P. Duarte, R. Martínez and L. J. Hoyos, *Ind. Eng. Chem. Res.*, 2016, **55**, 54–63.

25 V. Dal Santo, C. Dossi, A. Fusi, R. Psaro, C. Mondelli and S. Recchia, *Talanta*, 2005, **66**, 674–682.

26 G. Kresse and J. Furthmüller, *Phys. Rev. B - Condens. Matter Mater. Phys.*, 1996, **54**, 11169–11186.

27 G. Kresse and J. Furthmüller, *Comput. Mater. Sci.*, 1996, **6**, 15–50.

28 A. Hjorth Larsen, J. Jørgen Mortensen, J. Blomqvist, I. E. Castelli, R. Christensen, M. Dułak, J. Friis, M. N. Groves, B. Hammer, C. Hargus, E. D. Hermes, P. C. Jennings, P. Bjerre Jensen, J. Kermode, J. R. Kitchin, E. Leonhard Kolsbjerg, J. Kubal, K. Kaasbjerg, S. Lysgaard, J. Bergmann Maronsson, T. Maxson, T. Olsen, L. Pastewka, A. Peterson, C. Rostgaard, J. Schiøtz, O. Schütt, M. Strange, K. S. Thygesen, T. Vegge, L. Vilhelmsen, M. Walter, Z. Zeng and K. W. Jacobsen, *J. Phys. Condens. Matter*, 2017, **29**, 273002.

29 J. J. Mortensen, K. Kaasbjerg, S. L. Frederiksen, J. K. Nørskov, J. P. Sethna and K. W. Jacobsen, *Phys. Rev. Lett.*, 2005, **95**, 1–4.

30 J. Wellendorff, K. T. Lundgaard, A. Møgelhøj, V. Petzold, D. D. Landis, J. K. Nørskov, T. Bligaard and K. W. Jacobsen, *Phys. Rev. B - Condens. Matter Mater. Phys.*, 2012, **85**, 32–34.

31 P. E. Blöchl, *Phys. Rev. B*, 1994, **50**, 17953–17979.

32 G. Kresse and D. Joubert, *Phys. Rev. B - Condens. Matter Mater. Phys.*, 1999, **59**, 1758–1775.

33 E. Araujo-Lopez, L. Joos, B. D. Vandegehuchte, D. I. Sharapa and F. Studt, *J. Phys. Chem. C*, 2020, **124**, 3171–3176.

34 J. P. Perdew, K. Burke and M. Ernzerhof, *Phys. Rev. Lett.*, 1996, **77**, 3865–3868.

35 S. Grimme, J. Antony, S. Ehrlich and H. Krieg, *J. Chem. Phys.*, , DOI:10.1063/1.3382344.

36 L. Prati and G. Martra, *Gold Bull.*, 1999, **32**, 96–101.

37 L. Prati and A. Villa, *Catalysts*, 2012, **2**, 24–37.

38 S. Lowell, J. E. Shields, M. A. Thomas and M. Thommes, *Characterization of Porous Solids and Powders: Surface Area, Pore Size and Density*, 2004.

39 A. Antony, C. Hakanoglu, A. Asthagiri and J. F. Weaver, *J. Chem. Phys.*, , DOI:10.1063/1.3679167.

40 W. T. Tysoe, R. M. Ormerod, R. M. Lambert, G. Zgrablich and A. Ramirez-Cuesta, *J. Phys. Chem.*, 1993, **97**, 3365–3370.

Graphical Abstract (for review)

Click here to access/download;Graphical Abstract (for review);Benzaldehyde octanal2.tif

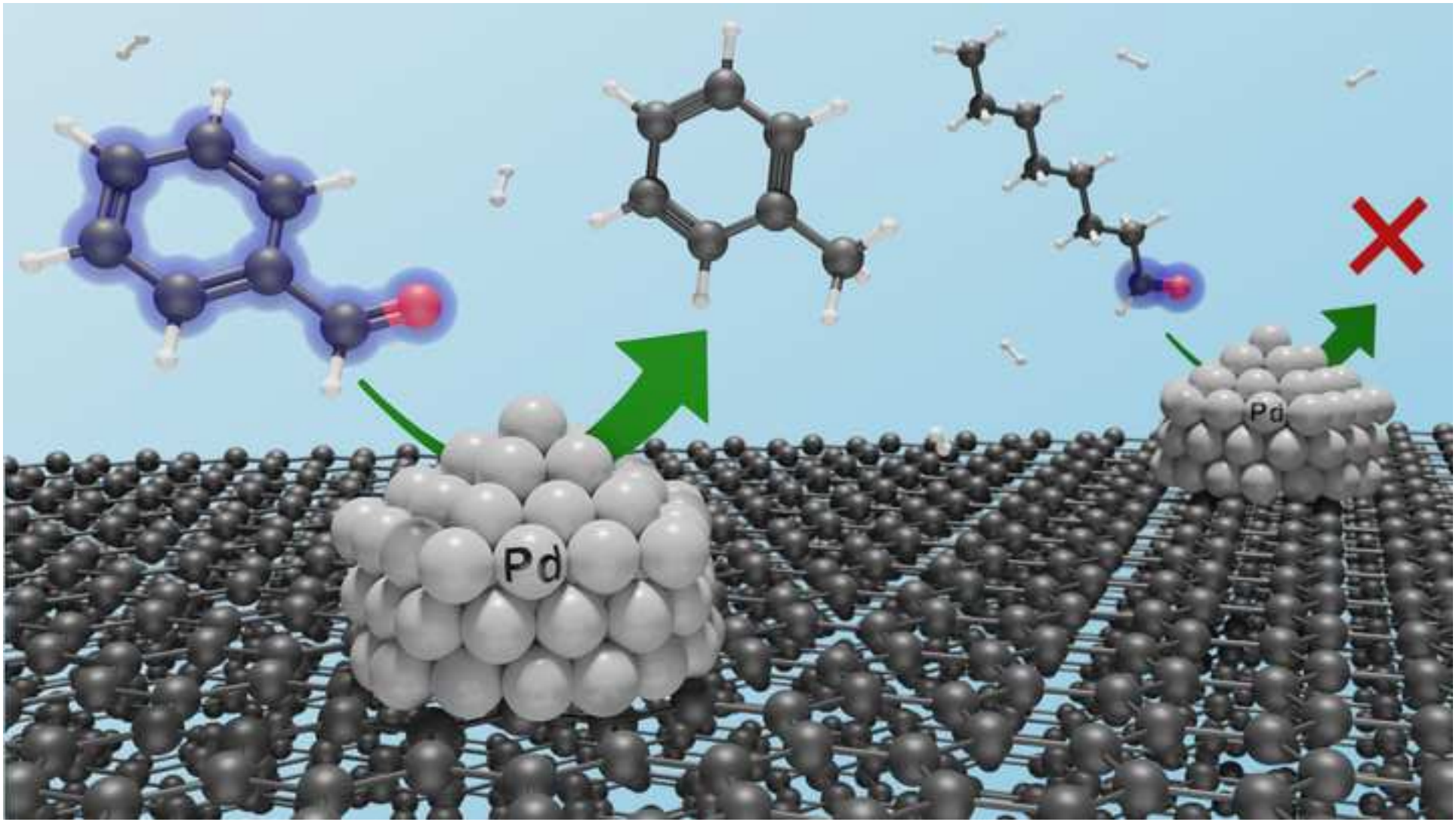

DISCOVERING THE ROLE OF SUBSTRATE IN ALDEHYDE HYDROGENATION

Stefano Cattaneo[a], Sofia Capelli[a], Marta Stucchi[a], Filippo Bossola[b], Vladimiro Dal Santo[b], Eduard Araujo-Lopez[c], Dmitry I. Sharapa[c], Felix Studt[c,d], Alberto Villa[a], Alessandro Chieregato[e], Bart D. Vandegehuchte[f] and Laura Prati[a,].*

[a] Dipartimento di Chimica, Università degli Studi di Milano, Via Golgi 19, 20133 Milano, Italy

[b] CNR – Istituto di Scienze e Tecnologie Chimiche "Giulio Natta", Via Golgi 19, 20133 Milano, Italy

[c] Institute of Catalysis Research and Technology, Karlsruhe Institute of Technology, Hermann-von-Helmholtz Platz 1, 76344 Eggenstein-Leopoldshafen, Germany

[d] Institute for Chemical Technology and Polymer Chemistry, Karlsruhe Institute of Technology, Engesserstrasse 18, 76131 Karlsruhe, Germany

[e] Total Research Center – Qatar (TRCQ), Qatar Science & Technology Park, Al Gharrafa, Doha P.O. Box 9803, Qatar

[f] Total Research & Technology Feluy, Zone Industrielle Feluy C, B-7181, Seneffe, Belgium

Highlights

- The importance of the side chain of aldehydes in determining the reactivity of carbonyl group was demonstrated
- Mode and strength adsorption are affected by the structure of the substrate, but these aspects are not the decisive factors
- Electronic activation via strong π-electron conjugation is key in the conversion of aldehydes to alcohols and hydrocarbons
- The study increases our knowledge on the mechanisms that govern heterogeneous catalysis

Keywords

Hydrogenation; hydrodeoxygenation; Pd; aromatic aldehyde; aliphatic aldehyde; adsorption; electron conjugation

SUPPLEMENTARY MATERIAL FOR: DISCOVERING THE ROLE OF SUBSTRATE IN ALDEHYDE HYDROGENATION

Stefano Cattaneo[a], Sofia Capelli[a], Marta Stucchi[a], Filippo Bossola[b], Vladimiro Dal Santo[b], Eduard Araujo-Lopez[c], Dmitry I. Sharapa[c], Felix Studt[c,d], Alberto Villa[a], Alessandro Chieregato[e], Bart D. Vandegehuchte[f] and Laura Prati[a,].*

[a] Dipartimento di Chimica, Università degli Studi di Milano, Via Golgi 19, 20133 Milano, Italy

[b] CNR – Istituto di Scienze e Tecnologie Chimiche "Giulio Natta", Via Golgi 19, 20133 Milano, Italy

[c] Institute of Catalysis Research and Technology, Karlsruhe Institute of Technology, Hermann-von-Helmholtz Platz 1, 76344 Eggenstein-Leopoldshafen, Germany

[d] Institute for Chemical Technology and Polymer Chemistry, Karlsruhe Institute of Technology, Engesserstrasse 18, 76131 Karlsruhe, Germany

[e] Total Research Center – Qatar (TRCQ), Qatar Science & Technology Park, Al Gharrafa, Doha P.O. Box 9803, Qatar

[f] Total Research & Technology Feluy, Zone Industrielle Feluy C, B-7181, Seneffe, Belgium

Hydrogenation/hydrodeoxygenation of aldehydes

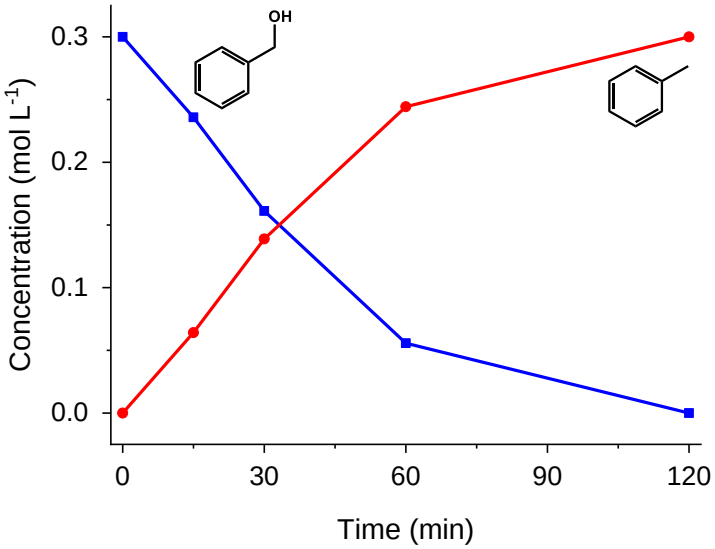

Figure S1: *Benzyl alcohol hydrodeoxygenation reaction. Reaction conditions: 50 °C, 2 bar of H_2, substrate-to-metal ratio 1000 : 1, benzaldehyde 0.3 mol L^{-1} in p-xylene.*

Computational Details

Benchmarking

Figure S1a shows the adsorption energies of C1-C8 alkanes on Pd(111) surface calculated using the BEEF-vdW and PBE-D3 functional compared to the experimental values as a function of the number of carbon atoms of the corresponding alkanes. The main interaction of these alkanes with the Pd(111) surface is stemming from dispersion forces and it can clearly be seen that the PBE-D3 functional is much better in reproducing the alkane adsorption energies compared to BEEF-vdW functional. In fact, PBE-D3 has only very small errors compared to the experiments. We therefore conclude that PBE-D3 is the best option for calculations of octanal adsorption and will use that for this purpose.

Figure S1b shows a comparison of the two functionals and the experimental adsorption energies of benzene on Pd(111) as a function of coverage. In this case, the situation is reversed: the BEEF-vdW functional is performing much better than PBE-D3, with the latter having an error of more than 70 kJ/mol. We therefore employed BEEF-vdW for calculations of the adsorption of benzaldehyde.

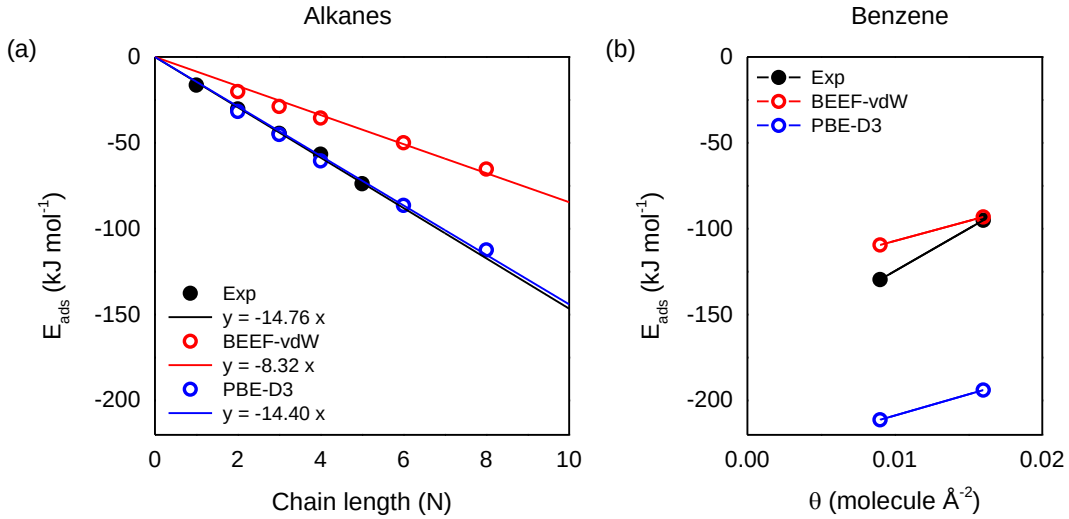

Figure S2: *The adsorption energy of (a) alkanes as a function of the carbon chain length, and (b) benzene as a function of surface coverage. Experimental values are taken from Antony et al. and Tysoe et al.*[1,2]

Variation of surface coverage

For the adsorption calculations, a four-layer slab of palladium with different supercell sizes of the surfaces and *k*-point meshes was used during the relaxation calculations. An overview is given in Table S1.

Table S1: *Adsorption energies (in kJ/mol) on the Pd(111) facet using the 4 layer slab model with the different cell sizes and corresponding k-point sampling.*

Surface	Area [Å^2]	*k*-points	Ethane	Propane	n-Butane	n-Hexane	n-Octane	Octanal	Benzene	Benzaldehyde
2×2	27.4	661	-	-	-	-	-	-89.0 (-97.7)	-	-53.9 (-77.6)
3×2	41.1	461	-	-	-	-	-	-85.0 (-113.4)	-	-66.2 (-125.9)
3×3	61.7	441	-20.6[a] (-32.0)[b]	-28.9 (-45.8)	-	-	-	-	-93.4 (-194.9)	-102.5 (-227.6)
3×6	123.4	421	-	-	-	-50.3 (-86.7)	-	-	-	-
3×7	144.0	411	-	-	-	-	-65.3 (-112.5)	-82.4 (-138.9)	-	-
4×4	109.7	331	-	-	-35.8 (-61.0)	-	-	-	-110.1 (-212.2)	-123.4 (-235.2)
4×5	137.1	321	-	-	-	-	-	-	-	-122.4 (-236.5)

[a] Full relaxation using BEEF-vdW functional.
[b] Single point values using PBE-D3 functional.

Electronic effect

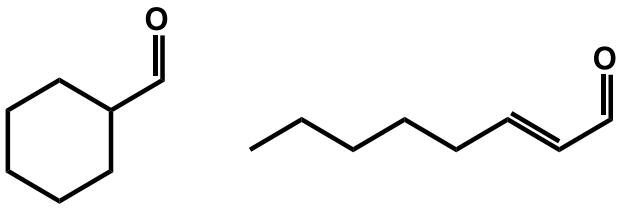

Cyclohexanecarboxyaldehyde **2-octenal**

Figure S3: *Molecular structure of cyclohexanecarboxyaldehyde and 2-octenal.*

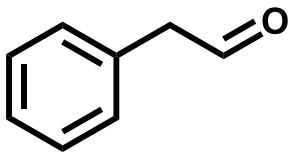

Figure S4: *Molecular structure of phenylacetaldehyde.*

References

1 W. T. Tysoe, R. M. Ormerod, R. M. Lambert, G. Zgrablich and A. Ramirez-Cuesta, *J. Phys. Chem.*, 1993, **97**, 3365–3370.

2 A. Antony, C. Hakanoglu, A. Asthagiri and J. F. Weaver, *J. Chem. Phys.*, 2012, **136**, 054702.